Mutual Coupling Effects Between Test and Reference Antennas in Near-Field Measurements

Scott G. H. Kriel and Dirk I. L. de Villiers

Abstract – This study considers near-field (NF) measurements performed by using a reference antenna to extract phase information from an unknown probe source. We simulate such a measurement of a prototype antenna element, designed for the proposed midfrequency aperture array of the Square Kilometre Array and attempt to transform the phase-extracted NF measurement into the far-field (FF) pattern of the antenna. The separation distance between the antenna under test and the reference antenna has a substantial effect on the resulting predicted FF pattern. Furthermore, this mutual coupling effect is found to be more pronounced in the NF region surrounding the antennas, leaving one to consider increasing the height of the scan plane to improve results. The analysis shows that one must carefully consider the effect that specific configurations have on NF measurements performed in this manner.

1. Introduction

The far-field (FF) radiation pattern of an antenna is a major consideration in the design and calibration of radio telescopes. Given the large scale of modern radio telescopes, such as the proposed midfrequency aperture array (MFAA) of the Square Kilometre Array, pattern verification via traditional methods becomes problematic. In light of this, there is interest in field measurements based on an unmanned aerial vehicle (UAV), whereby a UAV equipped with a transmitting source signal can be maneuvered throughout the observation domain of the antenna under test (AUT). This methodology is used in [1], where a UAV equipped with transmitting dipole antennas determines the FF pattern of various antenna systems. Here, the direct FF of the AUT is sampled, thus requiring the UAV to remain suitably far away in the FF region, commonly approximated as $r_{\text{far}} \geq 2D^2/\lambda$, where λ is the wavelength at the frequency in question and D is the maximum dimension of the antenna. This poses a problem when considering the MFAA, where the large aperture size of its various array stations (on the order of 50 m^2) may result in the FF region being located at distances that place unrealistic requirements on the UAV. This has led to the consideration of performing such UAV-based measurements in the near field (NF) of the AUT, whereby a suitable transform can be applied to calculate the required FF pattern. Although FF measurements only require the magnitude of the received power to be recorded, NF measurements require both amplitude and phase. The added necessity of measuring phase proves troublesome when considering a UAV-based system, as a common reference signal must be distributed between the probe and AUT for a relative phase measurement between the two to be performed. Although a direct cable link to the UAV may be realizable, as with the system proposed in [2], this will no doubt prove cumbersome in practice. We investigate a method in which a common reference signal can be established between the UAV and AUT in a detached fashion, using a reference antenna with well-known receiving characteristics. This phase reconstruction technique is performed in [3], which considers the practical UAV NF measurement of an aperture array. Although the article reports good agreement between the simulated and reconstructed phase of the AUT, no attempt is made at calculating the predicted FF pattern from the reconstructed data, as can be accomplished by using a suitable field transformation. Expanding on this topic, we first present a brief description of the fast irregular antenna field transformation algorithm (FIAFTA), which is subsequently used in a NF measurement simulation with a reference antenna to extract phase. Simulation of the problem illustrates how the position of the reference antenna relative to the AUT plays a vital role in the resulting accuracy of the predicted FF. Suspecting mutual coupling between the AUT and reference antenna as the main source of these discrepancies, we move on to analyze the extent to which the addition of a reference antenna serves to alter the NF of the AUT. Performing this for a number of measurement configurations, a suitable spacing between the AUT, reference, and probe antennas is established.

Manuscript received 26 August 2020.

Scott G. H. Kriel and Dirk I. L. de Villiers are with the Department of Electrical and Electronic Engineering, Stellenbosch University, 14 Bosman Street, Stellenbosch Central, Stellenbosch, 7600, South Africa; e-mail: scottkriel@gmail.com, ddv@sun.ac.za.

2. Field Transformation

To predict the FF pattern from the given NF measurements, a suitable transformation algorithm must be used. In this article, we use the FIAFTA developed and reviewed in [4]. Allowing for arbitrary sample locations, FIAFTA uses the diagonal translation operator T_L given as

$$T_L(\hat{k}, \hat{r}_M) = -\frac{jk}{4\pi} \sum_{l=0}^{L} (-j)^l (2l+1) \mathrm{h}_l^{(2)}(kr_M) \mathrm{P}_l(\hat{k} \cdot \hat{r}_M) \tag{1}$$

where $\mathrm{h}_l^{(2)}$ is the spherical Hankel function of the second kind and P_l a Legendre polynomial. The choice

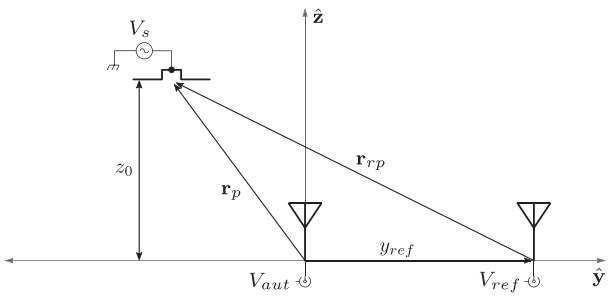

Figure 1. Schematic depicting NF measurement.

of multipole order L is made according to the electrical size of the AUT and is often taken to be $L = kd/2 + 10$, where d is the diameter of the smallest sphere enclosing the AUT and k is the wave number. In addition, T_L serves to translate outgoing plane waves from the AUT, emanating over all directions given by the wave vector $\mathbf{k} = k\hat{k}$, into incoming plane waves at the probe for each measurement location $\mathbf{r}_M = r_M\hat{r}_M$. The AUT is then replaced by a set of equivalent plane wave currents $\widetilde{\mathbf{J}}$ over the Ewald (or k space) sphere of the antenna [4]. Using T_L, these equivalent currents can be related to those of the probe, and the total response $\mathbf{U}$ is calculated by integrating the currents over the k-space sphere of the probe. Performing the integration via numerical quadrature, we can form the linear system of equations

$$\mathbf{U} = -j\frac{\omega\mu}{4\pi}||C|| \cdot \widetilde{\mathbf{J}} \tag{2}$$

where ω is the angular frequency of the wave and μ the permeability. The coupling matrix C is given as

$$C^{1/2}_{\theta/\phi}(\hat{k}, \hat{r}_M) = T_L(\hat{k}, \hat{r}_M)W(\hat{k}) \times P^{1/2}_{\phi/\theta}(\hat{k}, \hat{r}_M) \tag{3}$$

with $W(\hat{k})$ being the weighting function of the numerical integration scheme and $P^{1/2}_{\phi/\theta}$ denoting the θ- and ϕ-polarized receiving characteristics of probes 1 and 2 (measuring the copolarization and cross polarization, respectively). Using a suitable solver, such as the generalized minimal residual solver, one is able to solve for $\widetilde{\mathbf{J}}$, given a set of measured probe responses $\mathbf{U}$. With the determination of the set of equivalent plane wave currents of the AUT, one is able to approximate the FF $\mathbf{E}^{\mathrm{FF}}$ as

$$\mathbf{E}^{\mathrm{FF}}(r, \theta, \phi) = -j\frac{\omega\mu}{4\pi}\frac{e^{-jkr}}{r}\widetilde{\mathbf{J}}(k_\theta, k_\phi) \tag{4}$$

In addition to being used in the NF to FF transformation, this study also exploits FIAFTA in the proposed phase reconstruction via the reference antenna procedure. Note that the known FF pattern $\mathbf{E}^{\mathrm{FF}}$ of the reference antenna can be directly related to a set of equivalent plane wave currents $\widetilde{\mathbf{J}}$ by (4). Representing the reference antenna by this set of equivalent currents, one is able to calculate the response seen at the reference antenna $\mathbf{U}$ from (2) for specific probe and reference antenna positions. This calculated $\mathbf{U}$ can be regarded as the predicted complex response of the reference antenna for a measurement taken in the given configuration and with perfect phase retrieval (i.e., the source and received waves are sampled coherently). This predicted response can then be compared with that recorded for the actual measurement, so any phase differences between the predicted and measured responses caused by fluctuations in the source can be ascertained.

3. Measurement Configuration

The schematic in Figure 1 depicts the proposed configuration for a NF measurement by using a phase reference antenna. The AUT and reference antenna, with associated response signals V_{AUT} and V_{ref}, respectively, are separated along the y-axis by a distance y_{ref}. A probe, in the form of a source V_s attached to a transmitting dipole antenna, is then varied throughout the scan plane at constant height z_0 above the AUT. Fundamental to the premise of this study, we assume that the phase state of V_s is unknown and varies randomly throughout the measurement campaign. Aiming to recover this phase information, we record V_{AUT} and V_{ref} coherently, allowing for a relative phase measurement between the two. Focusing on specific application to the MFAA, we consider the log periodic dipole array prototype element developed by [5] as the AUT, which has a maximum dimension $D_{\mathrm{AUT}} = 0.46$ m. The broad pattern of such an antenna requires sampling relatively high power levels over a wide field of view (FoV). As such, the reference antenna must also be capable of receiving a decent signal over this FoV, and we choose a seven-element Yagi–Uda antenna to function as the reference antenna. The Yagi is designed with typical dimensions at a center frequency of 1 GHz and boom length of 1λ, giving a maximum dimension $D_{\mathrm{ref}} = 0.3$ m. From the outset, the spacing y_{ref} between the AUT and reference antenna and its effect on the resulting interference between the two was of concern. Attempting to gauge the extent to which the presence of the reference antenna affects the AUT, an x-polarized Yagi is placed at y_{ref} and passively terminated with a 50 Ω load impedance, while the AUT is excited by a 1 GHz source. Directly computing the FF pattern in Feko, version 2017.2 [6], we compare the results with and without the reference antenna placed at various positions y_{ref}. With respective NF regions approximated as $r_{\mathrm{near}} \leq 0.6$ m for the reference antenna and $r_{\mathrm{near}} \leq 1.4$ m for the AUT, we can expect some level of coupling to be present when one antenna is placed within the NF region of the other. Indeed, we find that a noticeable distortion in the AUT pattern can be seen when coupled to the Yagi placed at $y_{\mathrm{ref}} = 1$ m. The effect is most pronounced in the $\phi = 90°$ plane of the copolarized field (Figure 2) because the x-polarized AUT and reference antenna both exhibit a maximum beamwidth in the respective $\mathbf{H}$ planes, which happen to be aligned for the given measurement configuration. The value e_i contained in the legend is a scalar error metric, calculated

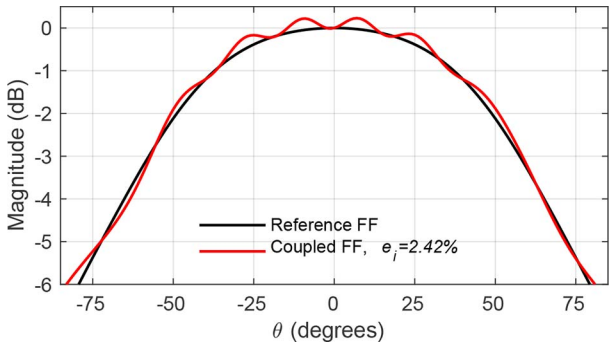

Figure 2. Direct FF patterns of the AUT in the $\phi = 90°$ plane when coupled to reference antenna placed at $y_{\text{ref}} = 1$ m.

by integrating the difference between the reference and coupled amplitude patterns over a 60° FoV. Increasing the spacing beyond $y_{\text{ref}} = 2$ m, we find that the extent of this distortion diminishes rapidly, becoming imperceptible when $y_{\text{ref}} = 4$ m. These results indicate that placing the reference antenna outside the NF region of the AUT sufficiently limits the distortion seen in the directly computed FF pattern. However, it remains to be seen whether such a condition holds true when considering NF to FF pattern prediction by using data obtained from the proposed NF measurement configuration.

4. Predicted FF Patterns

The proposed NF measurement is simulated in the given configuration by scanning the dipole probe through the measurement plane, while recording the complex voltage responses V_{AUT} and V_{ref}. A 5 m × 5 m scan plane is used, taken at a constant height $z_0 = 1$ m above the AUT. A sample spacing of $\Delta x = \Delta y = \lambda/2$ is used, and a uniform random phase is applied to V_s at each sample point in the simulation. By assuming no knowledge of this random source phase in the subsequent calculation of the FF, we replicate a practical measurement by using an isolated test source. Simulating the measurement with $y_{\text{ref}} = 1$ m, the predicted FF is considerably corrupted, again most notably in the $\phi = 90°$ plane, as shown by Figure 3 (top). This is not surprising as the direct FF calculation performed previously for Figure 2 indicated a significant amount of coupling at this separation distance. However, contrary to the direct FF calculation that showed minimal distortion for $y_{\text{ref}} = 4$ m, performing a NF measurement simulation at this separation distance still produced an unsatisfactory result, as shown in Figure 3 (bottom). Also included in the plots of Figure 3 is the predicted FF pattern for perfect phase reconstruction.

5. Mutual Coupling Investigation

The distortion seen in the predicted FF patterns is presumed to be caused by the reference antenna affecting the NF region of the AUT in some way. We move on to analyze the directly computed NF in the region around the AUT and reference antenna. More specifically, given that our previous findings show that

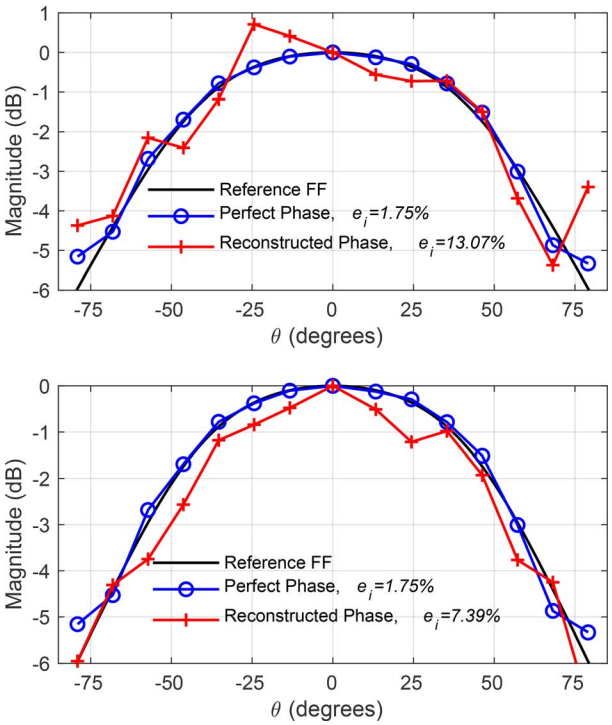

Figure 3. Transformed FF in the $\phi = 90°$ for NF measurements taken with probe height $z_0 = 1$ m and reference antenna at (top) $y_{\text{ref}} = 1$ m and (bottom) $y_{\text{ref}} = 4$ m.

the predicted patterns at $\phi = 90°$ are most severely affected, we consider the NF in the yz plane between $-5 \leq y \leq 5$ m and $1 \leq z \leq 6$ m. The AUT is then excited in the presence of the reference antenna, and the recorded NF is compared when the AUT is isolated. Furthermore, given that the receiving properties of the reference antenna also affect the FF prediction (in the phase extraction process), we repeat the experiment with the reference acting as a source, analyzing the effect the AUT has on its transmitted field. The error maps of these two measurements are then summed to yield a total error level, as given in Figure 4, showing the phase error with reference antenna at $y_{\text{ref}} = 1$ m. Low error levels are observed in the region, where each antenna

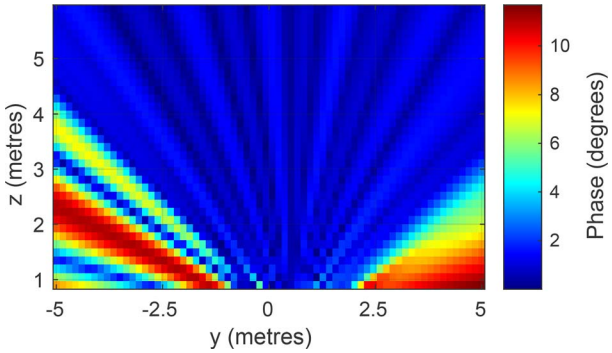

Figure 4. NF phase error in the yz plane, with reference antenna placed at $y = 1$ m.

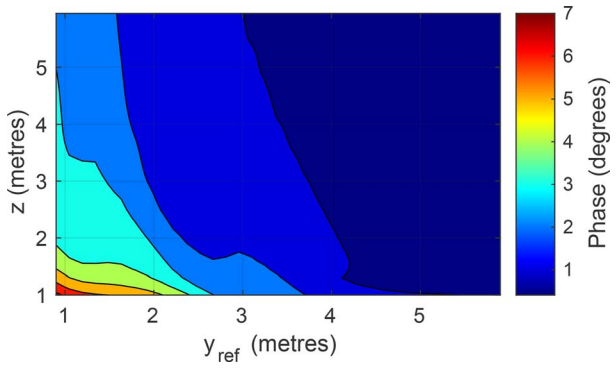

Figure 5. Contour plot showing the average NF phase error between $-5 \leq y \leq 5$ m, as a function of increasing height z above the AUT and position of reference antenna y_{ref}.

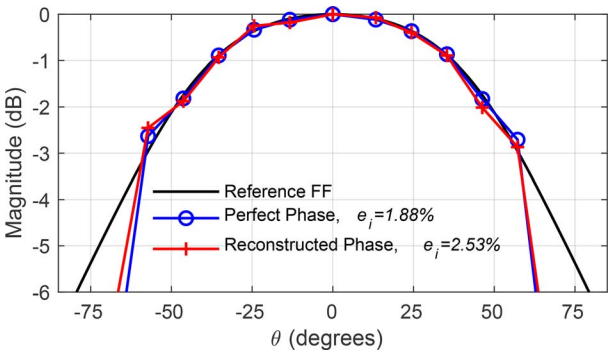

Figure 6. Transformed FF with $y_{\text{ref}} = 4$ m and $z_0 = 4$ m.

has a clear FoV, unobstructed by the presence of the other antenna. The errors encountered are more severe closer to the ground plane, where a phase error of over 10°, is observed. It is now clear that both the distance y_{ref} between the AUT and reference, together with the height z_0 of the chosen measurement plane, affect the phase-extracted NF measurement in question. To find suitable choices for both, we repeat the previously mentioned experiment 34 times, incrementally shifting the reference antenna by $\Delta y = \lambda/2 \approx 0.15$ m along the $\hat{y}$-axis between $1 \leq y_{\text{ref}} \leq 6$ m. For each measurement, we compute the average error seen along $-5 \leq y \leq 5$ m as a function of height z above the antennas. The results are combined in Figure 5, which shows the average phase error seen in the field as a function of height z above the antennas and separation distance y_{ref}. This contour plot shows how increasing z_0 and y_{ref} serves to reduce the incurred error in the NF. Informed by the previously mentioned investigation, we set up the measurement simulation with $z_0 = 4$ m and $y_{\text{ref}} = 4$ m. The resulting FF pattern for the $\phi = 90°$ plane is shown in Figure 6. It can be seen that increasing the separation distance y_{ref} between the AUT and reference antenna, as well as the height of the measurement plane z_0, serves to improve the results considerably.

6. Conclusion

The preceding analysis demonstrates the susceptibility of NF phase-extracted measurements to distortions caused by mutual coupling with a reference antenna. Accurate results when performing simulated NF measurements were dependent not only on the position of the reference antenna but also on the height of the scan plane. The choice of these two parameters determines the NF phase error encountered during the measurement. Given that this error is directionally dependent, the accuracy of the predicted FF will vary for different pattern cuts. As such, a low average NF phase error level calculated over the whole scan plane does not guarantee suitable performance in all predicted FF directions. This leads one to reconsider [3], where an average error in the NF phase between 7° and 13.5° is cited as having good agreement. However, as shown in the preceding analysis, NF phase errors on this level by no means ensure adequate FF prediction for all directions. Considering this, the verdict as to whether the phase reconstruction in [3] is adequate should be delayed until an attempt is made at predicting the FF pattern by using the reconstructed data.

7. Acknowledgment

This work is based on research supported by the National Research Foundation of South Africa (grant 75322).

8. References

1. P. Bolli, S. J. Wijnholds, E. de Lera Acedo, A. Lingua, J. Monari, et al., "In-Situ Characterization of International Low-Frequency Aperture Arrays by Means of an UAV-Based System," Thirty-Second General Assembly and Science Symposium of the International Union of Radio Science, Montreal, Quebec, Canada, August 19–26, 2017, pp. 1-4.
2. T. Fritzel, R. Strauss, H. Steiner, C. Eisner, and T. Eibert, "Introduction Into an UAV-Based Near-Field System for In-Situ and Large-Scale Antenna Measurements (Invited Paper)," IEEE Conference on Antenna Measurements & Applications, Syracuse, NY, USA, October 23–27, 2016, pp. 1-3.
3. L. Ciorba, G. Virone, F. Paonessa, S. Matteoli, P. Bolli, et al., "Near-Field Phase Reconstruction for UAV-Based Antenna Measurements," 2019 13th European Conference on Antennas and Propagation, Krakow, Poland, March 31–April 5, 2019, pp. 1-4.
4. T. F. Eibert, E. Kilic, C. Lopez, R. A. Mauermayer, O. Neitz, et al., "Electromagnetic Field Transformations for Measurements and Simulations," *Progress in Electromagnetics Research*, **151**, May 15, 2015, pp. 127-150, doi:10.2528/PIER14121105.
5. E. Colin-Beltran, A. J. Faulkner, and E. de Lera-Acedo, "Log-Periodic Sparse Aperture Array Antennas Dedicated to the MFAA Instrument of the SKA Telescope," International Conference on Electromagnetics in Advanced Applications, Palm Beach, Aruba, August 3–8, 2014, pp. 746-749.
6. Altair, "Altair Feko 2017.2," https://altairhyperworks.com/product/FEKO (Accessed June 16, 2019).